

Effect of Phosphines on the Thermodynamics of the Cobalt-Catalyzed Hydroformylation System

Robert J. Klingler,^{*,†} Michael J. Chen,[†] Jerome W. Rathke,[†] and Kurt W. Kramarz[‡]

Chemical Engineering Division, Argonne National Laboratory, 9700 South Cass Avenue, Argonne, Illinois 60439, and Oxo Alcohols & Plasticizers, BASF Corporation, 4403 La Porte Hwy. 225, Pasadena, Texas 77501

Received August 23, 2006

Thermodynamic parameters relevant to the phosphine-modified cobalt hydroformylation reaction are reported. Equilibrium constants for the hydrogenation of $\text{Co}_2(\text{CO})_8\text{L}_2$ to yield $\text{HCo}(\text{CO})_3\text{L}$ were determined using in situ ^1H and ^{31}P NMR spectroscopy between 75 and 175 °C for various solvents and phosphine ligands. Special emphasis was placed on $n\text{-Bu}_3\text{P}$, as this ligand is prototypical of the Shell hydroformylation process. The resultant van't Hoff plots yield the enthalpy and entropy change ($\Delta H = 7.0 \pm 0.4$ kcal/mol and $\Delta S = 2 \pm 1$ cal/mol·K) for the case of $\text{L} = n\text{-Bu}_3\text{P}$ in benzene solvent. These parameters were found to be relatively insensitive to changes in the solvent, suggesting that the hydride product is not very polar. Even for isobutyl alcohol solvent, the resultant enthalpy and entropy changes ($\Delta H = 5.8 \pm 0.4$ kcal/mol and $\Delta S = -2 \pm 1$ cal/mol·K) were found to be similar to those obtained in benzene and dioxane. Analysis of the ^{31}P NMR line widths allows rigorous lower limits to be established for the catalytically relevant Co–Co and Co–H bond energies in the case of $\text{L} = n\text{-Bu}_3\text{P}$ (Co–Co ≥ 23 kcal/mol and Co–H ≥ 60 kcal/mol) relative to the previously reported values for the case of $\text{L} = \text{CO}$ (Co–Co = 19 ± 2 kcal/mol and Co–H = 59 ± 1 kcal/mol).

Introduction

The hydroformylation of olefins to yield aldehydes and alcohols is one of the largest-scale industrial homogeneous catalytic processes.^{1,2} The products from this process are used in the manufacture of detergents, plastics, and agricultural products.³ While rhodium catalysts account for most of the C4 hydroformylation products, oxo reactions producing C5 and higher products are dominated by cobalt catalysts by a ratio of 9 to 1. The primary advantage of cobalt catalysts over rhodium is their higher reactivity toward internal olefins. Furthermore, the main advantage of the phosphine-modified cobalt hydroformylation system versus the unmodified cobalt catalysts is an improved yield of the desired linear product.³ The thermal stability of the phosphine-modified cobalt catalyst is desirable, as higher temperatures are required for separation of higher molecular weight products by distillation.²

We have been using high-pressure operando NMR spectroscopy within the various cobalt-catalyzed hydroformylation systems to characterize the key reaction intermediates while measuring the aldehyde production rates and organic product selectivity.^{4–8} The in situ NMR method can provide mechanistic insight that would be difficult to obtain by other means. For example, NMR spectroscopy has unique advantages for the investigation of systems with radical intermediates. Thus, the

$\text{Co}(\text{CO})_4$ radical concentration was measured as a function of temperature by NMR magnetic susceptibility measurements yielding the Co–Co bond energy for $\text{Co}_2(\text{CO})_8$. This was corroborated by a second well-established NMR method, contact shifting of the resonance for ligands entering the coordination sphere of a radical, which, in this case, was the carbonyl ligands. Both NMR methods consistently yield 19 ± 2 kcal/mol for the Co–Co bond energy, eq 1.⁶



The NMR methods are in good agreement with the latest mass spectroscopic observation, 20 ± 7 kcal/mol.⁹ In addition, there is high-pressure IR spectral evidence for the formation of $\text{Co}(\text{CO})_4$ radicals in n -hexane solution in the temperature range 120–210 °C.¹⁰ Interestingly, Hoff et al.¹¹ have pointed out that the $\text{Co}(\text{CO})_4$ radical concentrations that were determined by NMR spectroscopy are consistent with the rate of $\text{HCo}(\text{CO})_4$ production for the CO-independent pathway that was measured by Ungváry,¹² assuming that the trimolecular reaction process

(4) Rathke, J. W.; Klingler, R. J.; Krause, T. R. *Organometallics* **1991**, *10*, 1350–1355.

(5) Rathke, J. W.; Klingler, R. J.; Krause, T. R. *Organometallics* **1992**, *11*, 585–588.

(6) Klingler, R. J.; Rathke, J. W. *J. Am. Chem. Soc.* **1994**, *116*, 4772–4785.

(7) Kramarz, K. W.; Klingler, R. J.; Fremgen, D. E.; Rathke, J. W. *Catal. Today* **1999**, *49*, 339–352.

(8) Chen, M. J.; Klingler, R. J.; Rathke, J. W.; Kramarz, K. W. *Organometallics* **2004**, *23*, 2701–2707.

(9) Goebel, S.; Haynes, C. L.; Khan, F. A.; Armentrout, P. B. *J. Am. Chem. Soc.* **1995**, *117*, 6994–7002.

(10) Bor, G.; Dietler, U. K. IX International Conference on Organometallic Chemistry; September 3–7, 1979; Dijon, France, Abstracts: B56.

(11) Capps, K. B.; Bauer, A.; Kiss, G.; Hoff, C. D. *J. Organomet. Chem.* **1999**, *586*, 23–30.

(12) Ungváry, F. *J. Organomet. Chem.* **1972**, *36*, 363–370.

* Corresponding author. E-mail: klingler@cmt.anl.gov.

† Argonne National Laboratory.

‡ BASF Corporation.

(1) Collman, J. P.; Hegedus, L. S.; Norton, J. R.; Finke, R. G. *Principles and Applications of Organotransition Metal Chemistry*; University Science Books: Mill Valley, CA, 1987.

(2) Parshall, G. W.; Ittle, S. D. *Homogeneous Catalysis*; Wiley-Interscience: New York, 1992.

(3) Beller, M.; Cornils, B.; Frohning, C. D.; Kohlpainter, C. W. *J. Mol. Catal. A* **1995**, *104*, 17–85.

in eq 2 is proceeding near the diffusion-controlled limit,



as was found for the three examples in which the kinetics of such a radical process have been rigorously established. The underlying assumption is that trimolecular radical-based hydrogen activation processes will exhibit essentially no activation barrier, as long as the net reaction process is thermodynamically favorable. The enthalpy change for the reaction in eq 2 is quite favorable, $\Delta H = -14$ kcal/mol, on the basis of bond energy considerations using the Co–H bond energy, 59 kcal/mol, that was determined by NMR methods.⁶ At lower CO pressure, a faster CO-dependent pathway to the hydride becomes dominant.¹² The kinetics of the CO-dependent pathway have been investigated by Wegman and Brown, who found them to be consistent with a radical chain process that is catalyzed by Co(CO)₄.¹³ Both the CO-dependent and the CO-independent pathways for the production of HCo(CO)₄ involve the Co(CO)₄ radical. Our own unpublished kinetic data that were measured while determining the thermodynamics⁵ nicely corroborate Ungváry's results, as demonstrated in Figures 4 and 5 in the Supporting Information.

The Co(CO)₄ radicals that are produced by the thermolysis of Co₂(CO)₈ in eq 1 undergo facile hydrogen atom transfer reactions⁶ and have been proposed to promote many of the reactions of HCo(CO)₄ that are of central importance to the cobalt-catalyzed olefin hydroformylation process.¹⁴ Importantly, it has been shown that the reaction of HCo(CO)₄ with the type of unactivated olefins that are typically used in the hydroformylation reaction such as 1-hexene or 1-octene requires Co₂(CO)₈ promotion. The kinetic order in this very significant case was established and shown to be 0.5 order in Co₂(CO)₈.¹⁵ In contrast, activated olefins that are typified by styrene follow a different pathway involving a radical pair mechanism that is not influenced by the presence of Co₂(CO)₈.¹⁶ The ubiquitous 0.5 order in Co₂(CO)₈ that has been rigorously established^{13,15,17–19} in most of the cases involving unactivated substrates is difficult to reconcile with the conventional Heck–Breslow style reaction mechanism²⁰ for the hydroformylation reaction.^{20–24} Accordingly, despite the intense activity over the past 60 years on this important organocobalt system, further work on these reactions that involve the olefin substrate is strongly called for and will be investigated in more detail by the high-pressure operando NMR method in future studies.

The current work focuses on the effect of phosphine substitution on the thermodynamics for the key hydrogen activation step in eq 3,



where L = (*p*-CF₃C₆H₄)₃P and *n*-Bu₃P. In addition, it was hoped that the NMR measurements could shed some light on the effect of phosphine substitution on the strength of the Co–Co bond. In comparison with our previous measurement for L = CO, these phosphine ligands span a range of Lewis basicities and differ considerably in their back-bonding characteristics when compared with CO. Accordingly, data of this type should be of considerable value in providing experimental benchmarks for theoretical investigations of cobalt carbonyl hydride chemistry.^{25–30} The latter field spans an impressive range of reactions including the hydroformylation of olefins to aldehydes,^{21–23} the Reppe carbonylation of olefins to carboxylic acids,³¹ the homologation of methanol to higher alcohols,^{32–34} the BASF process for the carbonylation of methanol to acetic acid,² and the hydrogenation of CO to methanol.³⁵ The cobalt hydroformylation system based on the *n*-Bu₃P ligand was patented by Slauch and Mullineaux^{36,37} and is considered representative of the Shell hydroformylation process.^{22,36–39} We also report here on the solvent effect for hydride formation in eq 3 for this important phosphine ligand.

Experimental Section

Equilibrium reactions were examined in situ using a General Electric GN 300/89 NMR spectrometer equipped with a toroid detector pressure probe built in-house.⁴⁰ The pressure vessel portion of the probe was machined from Be–Cu alloy (Brush-Wellman alloy 25) and has an internal volume of 8 mL. Probe heating was accomplished by means of an outer-jacketed electrical furnace that fits snugly around the pressure vessel and is powered from a Sorensen DCR150-3B power supply and computer-controlled to within ± 0.1 °C using a copper-constantan thermocouple built into the furnace.

Equilibrium experiments were performed by initially loading solvents and cobalt complexes into the pressure vessel prior to assembly under a purified helium atmosphere in a glovebox. Reactive and/or inert gases were then admitted to the desired pressures. Pressures were monitored using a strain-gauge pressure transducer (Omega, model PX302-5KGV) and were controlled by means of an ISCO model 100DM high-pressure syringe pump. The

(13) Wegman, R. W.; Brown, T. *J. Am. Chem. Soc.* **1980**, *102*, 2494–2495.

(14) Pályi, G.; Ungváry, F.; Galamb, V.; Markó, L. *Coord. Chem. Rev.* **1984**, *37*–53.

(15) Ungváry, F.; Markó, L. *J. Organomet. Chem.* **1981**, *219*, 397–400.

(16) Ungváry, F.; Markó, L. *Organometallics* **1982**, *1*, 1120–1125.

(17) Ungváry, F.; Markó, L. *Organometallics* **1986**, *5*, 2341–2345.

(18) Ungváry, F.; Markó, L.; Bockman, T. M.; Garst, J. F.; King, R. B. *Isr. J. Chem.* **1986**, *27*, 262–266.

(19) Ungváry, F.; Sisak, A.; Markó, L. *Adv. Chem. Ser.* **1992**, *230*, 297–307.

(20) Heck, R. F.; Breslow, D. S. *J. Am. Chem. Soc.* **1961**, *83*, 4023–4027.

(21) Pino, P.; Piacenti, F.; Bianchi, M. In *Organic Synthesis via Metal Carbonyls*; Wender, I.; Pino, P., Eds.; Wiley: New York, 1977; Vol. 2, Chapter 2.

(22) Paulik, F. E. *Catal. Rev.* **1972**, *6*, 49–84.

(23) Orchin, M.; Rupilius, W. *Catal. Rev.* **1972**, *6*, 85–131.

(24) Pruet, R. L. *Advances in Organometallic Chemistry*; Stone, F. A., West, R., Eds.; Academic Press: New York, 1979; Vol. 17, pp 1–60.

(25) Versluis, L.; Ziegler, T. *Organometallics* **1990**, *9*, 2985–2992.

(26) Folga, E.; Ziegler, T. *J. Am. Chem. Soc.* **1993**, *115*, 5169–5176.

(27) Suderlin, L. S.; Dingneng, W.; Squires, R. R. *J. Am. Chem. Soc.* **1993**, *115*, 12060–12070.

(28) Barckholtz, T. A.; Bursten, B. E. *J. Organomet. Chem.* **2000**, *596*, 212–220.

(29) Huo, C.-F.; Li, Y.-W.; Wu, G.-S.; Beller, M.; Jiao, H. *J. Phys. Chem. A* **2002**, *106*, 12161–12169.

(30) Huo, C.-F.; Li, Y.-W.; Wu, G.-S.; Beller, M.; Jiao, H. *Organometallics* **2003**, *22*, 4665–4677.

(31) Weissmermel, K.; Arpe, H.-J. *Industrial Organic Chemistry*, 2nd ed.; VCH Publishers, Inc.: New York, 1993.

(32) Walker, W. E. U.S. Patent 4,277,634, 1981.

(33) Doyle, G. J. *J. Mol. Catal.* **1983**, *18*, 251–258.

(34) Koermer, G. S.; Slinkard, W. E. *Ind. Eng. Chem. Prod. Res. Dev.* **1978**, *17*, 231–236.

(35) Klingler, R. J.; Rathke, J. W. *Progr. Inorg. Chem.* **1991**, *39*, 113–180.

(36) Slauch, L. H.; Mullineaux, R. D., U.S. Patent 3,448,157, 1969.

(37) Slauch, L. H.; Mullineaux, R. D., U.S. Patent 3,448,158, 1969.

(38) Slauch, L. H.; Mullineaux, R. D. *J. Organomet. Chem.* **1968**, *13*, 469–477.

(39) Ibers, J. *J. Organomet. Chem.* **1968**, *14*, 423–428.

(40) Rathke, J. W.; Klingler, R. J.; Gerald, R. E., II; Kramarz, K. W.; Woelke, K. *Prog. Nucl. Magn. Reson. Spectrosc.* **1997**, *30*, 209–253.

Table 1. Spectroscopic Parameters

compound	IR, cm ⁻¹	³¹ P NMR, ppm
[Co(<i>n</i> -Bu ₃ P) ₂ (CO) ₃][Co(CO) ₄] ^a	1998 (s), 1982 (s), 1879 (vs) ^b	52.4
[Co(<i>n</i> -Bu ₃ P)(CO) ₃] ₂ ^c	1970 (s), 1950 (vs) ^d	53.7
HCo(<i>n</i> -Bu ₃ P)(CO) ₃ ^e	<i>f</i>	43.2
Co ₂ (<i>n</i> -Bu ₃ P)(CO) ₇ ^g	2078 (s), 2021 (s), 1992 (vs), 1954 (s)	56.0

^aReferences 41, 42. ^bReference 20. ^cReference 43. ^dReference 44. ^ePrepared by protonating the anion;⁴⁵ ¹H NMR [Co–H, –10.2 ppm (*J*_{H–P} = 47 Hz)].⁴⁶ ^fReference 42. ^gReference 47.

mixtures were allowed to stand for a period of 24 h after the probe was heated and thermally equilibrated to provide time for the gas phase to equilibrate with the liquid solvent. Reactions were monitored at constant temperature until no further changes were observed. In all cases observations were made while cycling the temperature up to some higher value and then back to the initial lower value to ensure the establishment of true equilibrium conditions by observing that the same concentrations were obtained in both cases.

Dicobalt octacarbonyl and tri-*n*-butylphosphine were purchased from Strem Chemicals Inc. and used without further purification. Phosphine-substituted cobalt carbonyl complexes were prepared from dicobalt octacarbonyl and tri-*n*-butylphosphine with modifications to previously reported methods. Standard Schlenk techniques with respect to handling air-sensitive compounds were followed. All solvents were purchased from Aldrich and were anhydrous, packed under nitrogen in Sure/Seal bottles, and used without further purification. Exceptions were benzene-*d*₆ and cyclohexane, which were used after degassing via freeze/pump/thaw cycles at –78 °C. All gases used were purchased from AGA Gas, Inc., and were at least 99.99% purity.

The preparations of the compounds followed literature procedures and are described elsewhere.⁷ In all cases we confirmed the literature values for the IR data. The ³¹P NMR chemical shift data were determined employing an external H₃PO₄ standard. For convenience, the relevant spectroscopic data are collected in Table 1.

Results

The hydrogenation of Co₂(CO)₆(*n*-Bu₃P)₂ was performed under mixtures of hydrogen and carbon monoxide in solvents of different polarity, eq 3. The reaction is sufficiently slow at ambient temperature such that all equilibrium measurements were conducted at temperatures above 100 °C. The hydride product is readily evident in both the ¹H and ³¹P NMR spectra. In benzene-*d*₆, the resonances of HCo(*n*-Bu₃P)(CO)₃ occur at 43.2 ppm in the ³¹P NMR spectra and –10.2 ppm (*J*_{H–P} = 47 Hz) in the ¹H NMR spectra. These resonances are not observed in the absence of hydrogen. Furthermore, these values are consistent with those obtained for samples of the hydride prepared by protonating the [Co(CO)₃(*n*-Bu₃P)][–] anion. Carbon monoxide reacts reversibly to affect the heterolytic Co–Co bond cleavage to yield the well-known mixed-valence salt indicated in eq 4,



which can be independently synthesized to confirm its chemical shift of 52.4 ppm. The process in eq 4 is reversible, and the thermodynamics have been determined.⁴⁸ High-pressure IR

(41) Imyanitov, N. S.; Volkov, V. A. *J. Gen. Chem. USSR (Engl. Transl.)* **1974**, *44*, 2741.

(42) Piacenti, F.; Andreatta, A.; Gregorio, G.; Montrasi, G.; Ferrari, G. *F. Chim. Ind.* **1967**, *49*, 245–252.

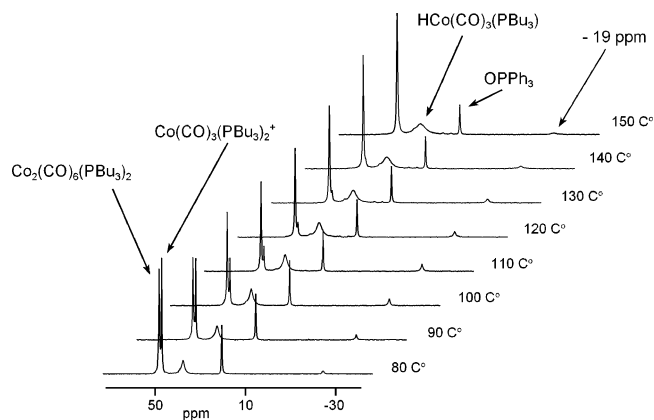
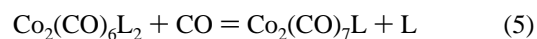


Figure 1. ³¹P NMR spectra for the reaction of Co₂(CO)₆(*n*-Bu₃P)₂ under CO and H₂.

investigations have suggested that the phosphine ligand is displaced by CO according to the equilibrium in eq 5.^{49–52}



In contrast to the IR investigations, the in situ NMR method found no detectable amount of Co₂(CO)₇(Bu₃P) formation under steady-state conditions with its unique chemical shift of 56.0 ppm even at 350 atm of CO pressure unless the Co/L ratio was less than unity.⁷ The Co₂(CO)₇(*n*-Bu₃P) complex is, however, observed as a transient species when the temperature is changed, as described in more detail in the Supporting Information. The Co₂(CO)₇(Bu₃P) complex is the major cobalt-containing component at a tributylphosphine loading of Co/L = 2.

The ³¹P NMR chemical shifts do not vary appreciably with solvent. Representative spectra for the hydrogenation of Co₂(CO)₆(*n*-Bu₃P)₂ in benzene solution employing a triphenylphosphine oxide internal reference are shown in Figure 1. It is apparent in Figure 1 that another species is observed at approximately –19 ppm. A discussion of what is currently known about the identity of this species can be found in the Supporting Information. The presence of this species does not adversely affect the hydride equilibrium measurements of this study.

It was not possible to investigate the reaction in eq 3 in a supercritical fluid phase for the case of *n*-Bu₃P. Thus, while Co₂(CO)₆(*n*-Bu₃P)₂ is soluble in supercritical carbon dioxide/toluene fluid, the salt that is produced by the reaction in eq 4 is not, and eventually all of the cobalt precipitates in this form.⁷ Therefore, it was not possible to directly obtain gas-phase equilibrium constants for this important ligand. Accordingly, the equilibrium constants that were measured for the reaction in eq 3 are *K_p* values with mixed standard states. The activity of the hydrogen is in units of atm, while those of the cobalt

(43) Manning, A. R. *J. Chem. Soc. A* **1968**, 1135–1137.

(44) Absi-Halabi, M.; Atwood, J. D.; Forbus, N. P.; Brown, T. L. *J. Am. Chem. Soc.* **1980**, *102*, 6248–6254.

(45) Hieber, W.; Lindner, E. *Chem. Ber.* **1961**, *94*, 1417–1425.

(46) Jesson, J. P. In *Transition Metal Hydrides*; Murtterties, E. L., Ed.; Marcel Dekker: New York, 1971; Chapter 4.

(47) Szabo, P.; Fekete, L.; Bor, G.; Nagy-Magos, Z.; Marko, L. *J. Organomet. Chem.* **1968**, *12*, 245–248.

(48) Rathke, J. W.; Klingler, R. J.; Chen, M. J.; Gerald, R. E., II; Kramarz, K. W. *Chemist* **2003**, *80*, 9–12.

(49) Bianchi, M.; Benedetti, E.; Piacenti, F. *Chim. Ind.* **1969**, *51*, 613–615.

(50) Whyman, R. *J. Organomet. Chem.* **1974**, *66*, C23–C25.

(51) Whyman, R. *J. Organomet. Chem.* **1974**, *81*, 97–106.

(52) van Boven, M.; Alemdaroglu, N.; Penninger, J. M. L. *J. Organomet. Chem.* **1975**, *84*, 65–74.

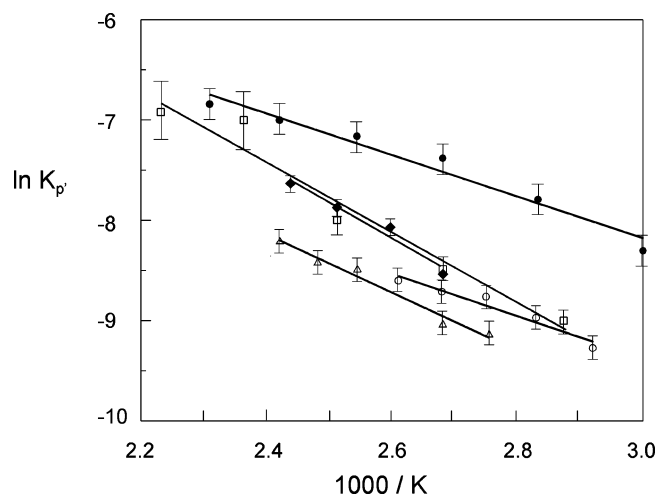


Figure 2. Van't Hoff plot for the hydrogenation of $\text{Co}_2(\text{CO})_6\text{L}_2$: ●, L = CO in scCO_2 ; □, L = $n\text{-Bu}_3\text{P}$ in benzene; ◆, L = $n\text{-Bu}_3\text{P}$ in dioxane; △, L = $n\text{-Bu}_3\text{P}$ in isobutyl alcohol; ○, L = $(p\text{-CF}_3\text{C}_6\text{H}_4)_3\text{P}$ in scCO_2 .

Table 2. Thermodynamic Parameters for the Hydrogenation of $\text{Co}_2(\text{CO})_6\text{L}_2^a$

solvent	ligand	ΔH° , kcal/mol	ΔS° , cal/(mol·K)
benzene	$n\text{-Bu}_3\text{P}$	7.0 (\pm 0.4)	2.0 (\pm 1.0)
dioxane ^b	$n\text{-Bu}_3\text{P}$	7.0 (\pm 0.7)	2.0 (\pm 1.7)
isobutyl alcohol	$n\text{-Bu}_3\text{P}$	5.8 (\pm 0.4)	-2.0 (\pm 1.0)
scCO_2	$(p\text{-CF}_3\text{C}_6\text{H}_4)_3\text{P}$	4.2 (\pm 0.6)	-6.1 (\pm 1.2)

^a The activity of the hydrogen is in units of atm, while those of the cobalt complexes are in concentrations, M. ^bPreviously reported.⁵³

complexes are in concentrations, M. For consistency, the results for the $(p\text{-CF}_3\text{C}_6\text{H}_4)_3\text{P}$ -substituted complex are also expressed in the same K_p' units despite the fact that the reaction was run in supercritical carbon dioxide (scCO_2), in which it is possible to directly measure gas-phase K_p values where all of the activities of the species in eq 3 are expressed in units of atm. The resulting van't Hoff plots are given in Figure 2, and the thermodynamic parameters are listed in Table 2. In addition, one of the data sets from our previous investigation⁵ of $\text{Co}_2(\text{CO})_8$ has been included in Figure 2 for comparison with the phosphine-modified dimers.

Discussion

General Comparisons. The solvent effects in the hydrogenation of $\text{Co}_2(\text{CO})_6(n\text{-Bu}_3\text{P})_2$ are found to be quite small. The largest difference between the more polar isobutyl alcohol and the other two solvents lies mainly in the entropy term, as is evident by the vertical offset of the lines (□, ◆, and △) in Figure 2. The similarity in the enthalpy terms for the three solvents suggests that the $\text{HCo}(\text{CO})_3(n\text{-Bu}_3\text{P})$ product in eq 3 is not very polar.⁵⁴ Similarly, the comparison of $\text{Co}_2(\text{CO})_8$ with the phosphine-substituted dimers in Figure 2 indicates that all of the systems are quite similar in terms of their enthalpies. The formation of $\text{HCo}(\text{CO})_4$ is favored over the $\text{HCo}(\text{CO})_3\text{L}$ products throughout the temperature range of interest for the hydroformylation reaction. Qualitatively, one of the largest differences

(53) Rathke, J. W.; Kramarz, K. W.; Klingler, R. J.; Chen, M. J.; Fremgen, D. E.; Gerald, R. E., II. *Trends Organomet. Chem.* **1999**, 3, 201–209.

(54) One of the referees has commented that the less endothermic enthalpy and negative reaction entropy in isobutyl alcohol may indicate that there is H-bonding between the OH moiety of the solvent molecule with the hydride ligand of $\text{HCo}(n\text{-Bu}_3\text{P})(\text{CO})_3$.⁵⁵

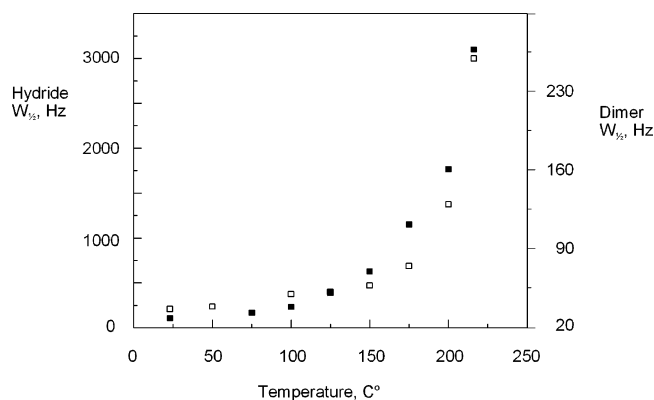


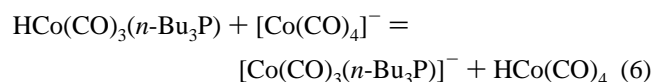
Figure 3. Temperature dependence of the ^{31}P NMR line widths: □, $\text{Co}_2(\text{CO})_6(n\text{-Bu}_3\text{P})_2$; ■, $\text{HCo}(\text{CO})_3(n\text{-Bu}_3\text{P})$.

between the sterically demanding $n\text{-Bu}_3\text{P}$ ligand and CO lies in the entropy term, as is evident from the vertical offset between the lines in Figure 2. More detailed discussion of the thermodynamics follows in a subsequent section after the mixed-phase data in Table 1 are converted into gas-phase values.

Line Widths in the ^{31}P NMR Spectra. The ^{31}P NMR resonances for $\text{HCo}(\text{CO})_3(n\text{-Bu}_3\text{P})$ and $\text{Co}_2(\text{CO})_6(n\text{-Bu}_3\text{P})_2$ in Figure 1 broaden with temperature in a highly correlated manner, as demonstrated in Figure 3, where they are plotted in the same graph but employing different vertical scales. This behavior is reminiscent of the hydrogen atom transfer chemistry that was observed in the parent $\text{Co}_2(\text{CO})_8$ system.⁶ The atom-transfer chemistry equilibrates the cobalt centers in the hydride and dimer.

Accordingly, the dynamics of the hydride and the dimer are coupled by a single reaction sequence in the parent $\text{Co}_2(\text{CO})_8$ system. Alternatively, if the hydride and the dimer in the phosphine-substituted system are reacting by two completely independent processes, then the activation parameters for these two unrelated processes must be fortuitously similar, as the ratio of the two rates (first-order lifetimes) in Figure 3 are nearly invariant with temperature. Possibilities for independent processes include proton transfer, hydride transfer, Berry pseudorotation, and phosphorus ligand exchange.

Proton transfer between the hydride and the tetracarbonyl anion from the salt that is produced by the reaction in eq 4,



is an unlikely candidate for the dynamic process, as the reaction in eq 6 is predicted to be thermodynamically uphill by more than 7 $\text{p}K_a$ units. The $\text{p}K_a$ of $\text{HCo}(n\text{-Bu}_3\text{P})(\text{CO})_3$ has not been reported in the literature; however, the $\text{p}K_a$ of $\text{HCo}(\text{CO})_4$ in acetonitrile is 8.3 and the $\text{p}K_a$ of the triphenylphosphine hydride analogue, $\text{HCo}(\text{Ph}_3\text{P})(\text{CO})_3$, is 15.4.^{56,57} Accordingly, the $\text{p}K_a$ of $\text{HCo}(n\text{-Bu}_3\text{P})(\text{CO})_3$ can be approximated as 18 given the difference in $\text{p}K_a$ of Ph_3P and $n\text{-Bu}_3\text{P}$ and the reported effects of phosphine basicity on transition metal phosphine hydrides.^{58,59}

(55) Crabtree, R. H.; Siegbahn, P. E. M.; Eisenstein, O.; Rheingold, A. L.; Koetzle, T. F. *Acc. Chem. Res.* **1996**, 29, 348–354.

(56) Moore, E. J.; Sullivan, J. M.; Norton, J. R. *J. Am. Chem. Soc.* **1986**, 108, 2257–2263.

(57) Tilset, M.; Parker, V. D. *J. Am. Chem. Soc.* **1989**, 111, 6711–6717.

(58) Kristjánjansdóttir, S. S.; Norton, J. R. In *Transition Metal Hydrides: Recent Advances in Theory and Experiment*; Dedieu, A., Ed.; VCH: New York, 1992; pp 309–359, and references therein.

(59) Masters, C. *Homogeneous Transition-Metal Catalysts—A Gentle Art*; Chapman and Hall: London, 1981; p 116, and references therein.

A second argument against proton transfer is that the concentration of $[\text{Co}(\text{CO})_3\text{L}_2][\text{Co}(\text{CO})_4]$ decreases rapidly with temperature because the reaction in eq 4 is strongly exothermic.⁴⁸ In contrast, the broadening of $\text{HCo}(\text{Bu}_3\text{P})(\text{CO})_3$ progressively increases with temperature (Figure 3). One of the strongest arguments against proton transfer is that it is hard to envision why the dimer would be directly involved in any proton-transfer scheme, let alone have an activation parameter similar to that for the hydride. Similarly, hydride transfer from $\text{HCo}(n\text{-Bu}_3\text{P})(\text{CO})_3$ to the cation $[\text{Co}(n\text{-Bu}_3\text{P})_2(\text{CO})_3]^+$ from eq 4 is unlikely given that the observed line width of the ^{31}P NMR resonance attributed to this cation at 52.2 ppm does not broaden as the hydride resonance does.

Another potential explanation for the broadening of the ^{31}P NMR resonances is the Berry pseudorotation dynamic process, which is well established for five-coordinate cobalt complexes similar to those in this system.⁴⁶ Thus, the pseudorotation process has been observed for directly analogous alkyl complexes. However, the fast exchange limit is typically reached at much lower temperatures than those shown in Figure 3. Furthermore, the activation energy apparent in Figure 3 is much higher than that typically observed for Berry pseudorotation.⁴⁶

The possibility of two completely independent phosphine ligand exchange pathways is more difficult to exclude. Increased CO pressure does not sharpen the hydride resonance. Likewise, adding excess $n\text{-Bu}_3\text{P}$ to the system does not alter the broadening of the hydride at higher temperatures. Unfortunately, this result is somewhat ambiguous because the species at -19 ppm reacts with phosphine and is always in fast exchange with free phosphine at these temperatures. Accordingly, one cannot determine how much free phosphine there is under the reaction conditions shown in Figure 3. Perhaps the strongest argument against two independent ligand exchange pathways is that the data in Figure 3 would require that phosphine exchange with the dimer and the hydride must be proceeding with nearly the same activation energy because the ratio of the two rates is invariant with temperature.

Alternatively, it is easy to envision phosphine exchange as being an integral part of an atom-transfer mechanism based on $\text{Co}(\text{CO})_3\text{L}$ radicals and that such a modification over the parent $\text{Co}_2(\text{CO})_8$ system⁶ could explain why the hydride resonance is always an order of magnitude broader than that of the dimer in the phosphine-modified system. In contrast, the dimer and the hydride broadened in a symmetrical fashion within the parent system.⁶ However, lacking unequivocal evidence for radicals in the phosphine-substituted system, it seems unwarranted to present mechanistic schemes based on radical intermediates at present.

Effect of Phosphines on the Co–Co Bond Energy. As noted above, the data in Figure 3 are highly reminiscent of the hydrogen atom transfer chemistry that was observed in the parent $\text{Co}_2(\text{CO})_8$ system. However, to rigorously establish this point and to elucidate all of the chemistry in the phosphine-substituted system would require directly measuring the radical concentration as was done in the parent $\text{Co}_2(\text{CO})_8$ system. The data in Figure 3 demonstrate that it would require measurements in the 225–275 °C temperature range to generate sufficiently high radical concentrations to be detectable by the NMR magnetic susceptibility method. Furthermore, the $n\text{-Bu}_3\text{P}$ will not survive those conditions, as Hoffman degradation is already evident in the ^{31}P NMR spectra (doublets originating from the formation of P–H moieties) at temperatures above 200 °C. Alternatively, the ^{13}CO NMR contact shift method gave the

same Co–Co bond energy as the NMR magnetic susceptibility method in the $\text{Co}_2(\text{CO})_8$ system.⁶ In addition, we have qualitatively observed the same type of shifting of the free ^{13}CO resonance in the $\text{Co}_2(\text{CO})_6(n\text{-Bu}_3\text{P})_2$ system at temperatures below 200 °C. The contact shift NMR method is more sensitive to lower radical concentration levels. However, both of these NMR methods would probably be best done employing a more thermally stable phosphine such as alkylated phobane.⁶⁰

Despite the above qualifications, the data in Figure 3 do allow some conclusions to be drawn about the effect of phosphine substitution on the Co–Co bond energy. The lifetimes of the phosphine centers in the $\text{Co}_2(\text{CO})_6(n\text{-Bu}_3\text{P})_2$ complex place a rigorous upper limit on the rate of Co–Co bond dissociation. Accordingly, the Co–Co bond is stronger in both of the phosphine-substituted compounds than that for $\text{Co}_2(\text{CO})_8$. For example, the lifetime of the $n\text{-Bu}_3\text{P}$ moiety in $\text{Co}_2(\text{CO})_6(n\text{-Bu}_3\text{P})_2$, metered by its change in ^{31}P NMR line width $\Delta W_{1/2}$, is longer than that of the cobalt center in $\text{Co}_2(\text{CO})_8$, metered by its change in ^{59}Co NMR line width $\Delta W_{1/2}$, by 2 orders of magnitude at 200 °C. This difference in rates translates into 4 kcal/mol. The Co–Co bond in $\text{Co}_2(\text{CO})_6(n\text{-Bu}_3\text{P})_2$ is stronger than that in $\text{Co}_2(\text{CO})_8$ by at least 4 kcal/mol or $\text{Co–Co} \geq 23$ kcal/mol.

Before discussing the energetics of the Co–H bond we would like to address a more general question of how one might convert mixed-phase equilibrium constants of the type in Table 2 into true gas-phase values that can then be compared with the ones generated by computational methods. In the next section, we suggest a method that seems applicable where it has been shown that the solvent effects, Table 2, are small.

Gas-Phase Thermodynamics. The type of mixed-phase K_p' values measured in this study are not true gas-phase equilibrium K_p values. The two types of equilibrium constants are not based on the same set of standard states and, in most cases, will not even have the same units. However, the mixed-phase K_p' values are usually easier to measure, while the gas-phase K_p values are more desirable for comparison with results from theoretical calculations. This raises the question whether it is possible to convert the measured mixed-phase K_p' values into the desired gas-phase K_p values.

Previously we have noted that our K_p' values that were measured for the hydrogenation of $\text{Co}_2(\text{CO})_8$ in supercritical carbon dioxide⁵ were very close to those previously measured in solution phase by Ungváry.¹² Recently, a new set of solution-phase data has become available, and it was noted in that study that the K_p' data from all of the sources were sufficiently consistent that all of it could be combined and fit with a single linear regression.⁶¹ The small solvent effect for $\text{Co}_2(\text{CO})_6(n\text{-Bu}_3\text{P})_2$ in Table 2 suggests that this will likely be a good approximation for the $\text{Co}_2(\text{CO})_6\text{L}_2$ complexes as well. Accordingly, to the extent it can be assumed that a K_p' value measured under mixed-phase gas/solution reaction conditions will have the same K_p' value as that measured for the same reagents under single-gas-phase reaction conditions, such as in scCO_2 , it is easy to obtain the desired gas-phase K_p values. Thus, the assumption that the measured mixed-phase K_p' values are equal to the gas-phase K_p values, and that the ideal gas law can be used to convert the resulting gas-phase K_p' values into gas-phase K_p

(60) Eberhard, M. R.; Carrington-Smith, E.; Drent, E. E.; Marsh, P. S.; Prpen, A. G.; Phetmung, H.; Pringle, P. G. *Adv. Synth. Catal.* **2005**, *347*, 1345–1348.

(61) Tannenbaum, R.; Dietler, U. K.; Bor, G.; Ungváry, F. *J. Organomet. Chem.* **1998**, *570*, 39–47.

Table 3. Thermodynamic Parameters for the Hydrogenation of $\text{Co}_2(\text{CO})_6\text{L}_2$ Adjusted to Gas-Phase Conditions^a

solvent	ligand	ΔH° , kcal/mol	ΔS° , cal/(mol·K)
benzene	<i>n</i> -Bu ₃ P	7.8 (± 0.4)	11 (± 1.0)
dioxane ^b	<i>n</i> -Bu ₃ P	8.0 (± 0.7)	11 (± 1.7)
isobutyl alcohol	<i>n</i> -Bu ₃ P	6.6 (± 0.4)	7 (± 1.0)
scCO ₂	(<i>p</i> -CF ₃ C ₆ H ₄) ₃ P	4.9 (± 0.6)	2 (± 1.2)
scCO ₂ ^c	CO	4.7 (± 0.2)	4.4 (± 0.5)

^a The activity of all of the species are in units of atm using the conversion $K_p = (RT)K_p'$ as described in the text. ^bReference 53. ^cReference 5.

values, yields the following relationship for the stoichiometry of the systems reported in this work:

$$K_p = (RT)K_p'$$

Regardless of the accuracy of the underlying assumptions, at the very least, this relationship will convert the measured K_p' values into the proper units for gas-phase K_p values. This relationship was used to convert the enthalpy/entropy values in Table 2 that were obtained from the K_p' measurements observed under mixed-phase reaction conditions into the gas-phase enthalpy/entropy values listed in Table 3.⁶² The assumptions really only apply to *n*-Bu₃P, as the other values were directly measured in a fluid phase, scCO₂.

A comparison of the first and last rows of Table 3 indicates that the enthalpy of hydrogenation of $\text{Co}_2(\text{CO})_6(\textit{n}\text{-Bu}_3\text{P})_2$ is 3 kcal/mol less favorable than it is for $\text{Co}_2(\text{CO})_8$. In addition, the Co–Co bond in the substituted dimer is at least 4 kcal/mol stronger than that for dicobalt octacarbonyl. These effects nearly cancel. Accordingly, the Co–H bond is stronger in $\text{HCo}(\text{CO})_3\text{L}$ than it is in $\text{HCo}(\text{CO})_4$. However, the difference may be quite small. Thus, the Co–H bond energy in the phosphine-substituted hydride is greater than 60 kcal/mol versus 59 ± 1 for $\text{HCo}(\text{CO})_4$. This observation is consistent with previous results where the Co–H bond energy in $\text{HCo}(\text{CO})_4$ was found to be quite similar to that in $\text{HCo}(\text{CO})_3\text{PPh}_3$.⁶³ The previous work was conducted by a combined electrochemical/acidity method that leads to Co–H bond energies that are consistently about 8 kcal/mol higher than the NMR⁶ result for the Co–H bond energy and recent mass spectrometric value⁹ for the Co–Co bond energy.⁶⁴ Similarly other work investigating the effect of oxidation state on the Co–H bond energy has shown that the changes with increasing charge are minor.⁶⁶

One of the largest differences in Table 3 between the sterically demanding *n*-Bu₃P ligand and CO lies in the entropy term. A case can be made that both the direction and the magnitude of this difference in entropy are consistent with previous work. Thus, the M–M bond dissociation entropy has been measured

(62) Tabulations of the K_p' and K_p data are contained in Table 4 in the Supporting Information.

(63) (a) Tilset, M.; Parker, V. D. *J. Am. Chem. Soc.* **1989**, *111*, 6711–6717. (b) Tilset, M.; Parker, V. D. *J. Am. Chem. Soc.* **1990**, *112*, 2843.

(64) The Co–Co bond energy is linked to the Co–H bond energy by the enthalpy change for the hydrogenation of the dimer. This latter quantity has been investigated independently by three groups with excellent agreement.^{5,12,61} (See ref 61 for a discussion of a fourth observation that is inconsistent with the other three.) Accordingly, if the Co–H bond energy is 8 kcal/mol higher, then the Co–Co bond energy must be 16 kcal/mol higher, placing it at 35 kcal/mol. This 35 kcal/mol value is well outside the error range of either the NMR measurement, 19 ± 2 kcal/mol,⁶ or the latest mass spectroscopic value, 20 ± 7 kcal/mol.⁹ Furthermore, 35 kcal/mol is much higher than any of the measurements for the Co–Co bond energy, some of which were as low as 14.5 kcal/mol.⁶⁵

(65) Simoes, J. A. M.; Beauchamp, J. L. *Chem. Rev.* **1990**, *90*, 629–688.

(66) Ciancanelli, R.; Noll, B. C.; DuBois, D. L.; DuBois, M. R. *J. Am. Chem. Soc.* **2002**, *124*, 2984–2992.

for a number of dimers and lies in the range 30–45 cal/(mol·K).^{67,68} This entropy term increases rapidly with the steric requirements of the ligands attached to the metal center.⁶⁸ Furthermore, the entropy change for Co–Co bond dissociation in $\text{Co}_2(\text{CO})_8$, $\Delta S = 29 \pm 4$ cal/(mol·K),⁶ lies at the lower end of this range. The data in Table 3 are consistent with phosphine substitution increasing the M–M bond dissociation entropy due to steric effects.

Conclusions

The thermodynamics for the hydrogenation of $\text{Co}_2(\text{CO})_6\text{L}_2$ to yield $\text{HCo}(\text{CO})_3\text{L}$ were determined using in situ ¹H and ³¹P NMR spectroscopy between 75 and 175 °C for various solvents and phosphine ligands. These parameters were found to be relatively insensitive to changes in the solvent for the prototypical Shell catalyst, *n*-Bu₃P, suggesting that the hydride product is not very polar. Similarly, the parent $\text{Co}_2(\text{CO})_8$ system was found to be quite similar to the phosphine-substituted dimers with L = *n*-Bu₃P and (*p*-CF₃C₆H₄)₃P. The formation of $\text{HCo}(\text{CO})_4$ is favored over the $\text{HCo}(\text{CO})_3\text{L}$ products throughout the temperature range of interest for the hydroformylation reaction. Analysis of the ³¹P NMR line widths allows rigorous lower limits to be established for the catalytically relevant Co–Co and Co–H bond energies in the case of L = *n*-Bu₃P (Co–Co ≥ 23 kcal/mol and Co–H ≥ 60 kcal/mol) relative to the previously reported values for the case of L = CO (Co–Co = 19 ± 2 kcal/mol and Co–H = 59 ± 1 kcal/mol).

A method has been suggested for converting mixed-phase gas/solution equilibrium data into gas-phase values in systems where the reaction has been shown to exhibit minimal solvents effects. This type of conversion should facilitate the comparison of experimental metal–metal and metal–hydride bond energies to those computed from DFT calculations.

The ³¹P resonances for $\text{HCo}(\text{CO})_3(\textit{n}\text{-Bu}_3\text{P})$ and $\text{Co}_2(\text{CO})_6(\textit{n}\text{-Bu}_3\text{P})_2$ broaden with temperature in a highly correlated manner. This behavior is highly reminiscent of the hydrogen atom transfer chemistry that was observed in the parent $\text{Co}_2(\text{CO})_8$ system. Measurement of the Co–Co bond energy in the phosphine-substituted system by NMR magnetic susceptibility and contact shift measurements will require studies in the 225–275 °C range to generate sufficient concentrations of radicals. This is not feasible with *n*-Bu₃P, but should be possible with more thermally stable phosphines such as alkylated phobane.

Acknowledgment. The authors thank Professor J. Halpern for helpful discussions. Support for this work was provided by the Office of Basic Energy Sciences, Division of Chemical Sciences, U.S. Department of Energy, under contract W-31-109-ENG-38.

Supporting Information Available: (1) Complete tabulation of the K_p and K_p' values, Table 4. (2) Integrated rate-law plots for the hydrogenation of $\text{Co}_2(\text{CO})_8$ to $\text{HCo}(\text{CO})_4$, Figure 4, and activation parameters for hydride formation, Figure 5. (3) Extended discussion of the formation of $\text{Co}_2(\text{CO})_7(\textit{n}\text{-Bu}_3\text{P})$ under transient temperature conditions. (4) Extended discussion of the characterization of the species with a ³¹P NMR resonance near –19 ppm. This material is available free of charge via the Internet at <http://pubs.acs.org>.

OM060768D

(67) Watkins, W. C.; Jaeger, T.; Kidd, C. E.; Fortier, S.; Baird, M. C.; Kiss, G.; Roper, G. C.; Hoff, C. D. *J. Am. Chem. Soc.* **1992**, *114*, 907–914.

(68) Hoff, C. D. *Coord. Chem. Rev.* **2000**, *206*, 451–467.